Laboratory Observations of Hall Magnetic Field in Electron-Only Magnetic Reconnection With a Guide Field

Fa Yang[1,2,3] ![ORCID], Quanming Lu[1,2,3] ![ORCID], Qiaofeng Zhang[1,2,3], Jinlin Xie[4], Xinliang Gao[1,2,3] ![ORCID], Yangguang Ke[1,2,3] ![ORCID], Lei Tang[1] ![ORCID], Shihang Hu[1], Yukang Shu[1] ![ORCID], Youran Liu[4], Longlong Sang[2], San Lu[1,2,3] ![ORCID], Rongsheng Wang[1,2,3] ![ORCID], and Weixing Ding[4]

[1]CAS Key Lab of Geospace Environment, School of Earth and Space Sciences, University of Science and Technology of China, Hefei, China, [2]Deep Space Exploration Laboratory, CAS Center for Excellence in Comparative Planetology, Hefei, China, [3]Collaborative Innovation Center of Astronautical Science and Technology, Harbin, China, [4]School of Nuclear Science and Technology, University of Science and Technology of China, Hefei, China

Abstract Recently, electron-only reconnection, in which there is no obvious ion bulk flow and ion heating, has been pervasively observed in the Earth's magnetosphere. In this Letter, we realize electron-only reconnection with a guide field in the Keda Linear Magnetized Plasma (KLMP) device. By measuring the magnetic field, we identify unambiguously a distorted quadrupolar structure of the magnetic field in the out-of-plane direction. At the same time, electrons are obviously heated in the current sheet with the half-width about 0.8 electron inertial length. The maximum velocity of the estimated electron flow in the reconnection plane is about eight Alfvén speed.

Plain Language Summary Magnetic reconnection, a fundamental process during which magnetic field lines break and reconfigure their connectivity, can convert magnetic energy into plasma kinetic and thermal energy in space and laboratory plasmas. A standard reconnection model with both ion and electron dynamics has been established to describe the magnetic reconnection observed in space and laboratory plasmas. Recently, a new type of magnetic reconnection has been pervasively observed in space, called electron-only reconnection, in which there is no obvious ion bulk flow and ion heating. Here, we realize electron-only reconnection experiments in the Keda Linear Magnetized Plasma (KLMP) device. By measuring the magnetic fields in a two-dimensional reconnection plane, we find that the magnetic field in the out-of-plane direction has a distorted quadrupolar structure. Additionally, electrons are obviously heated in a thin electron-scale current sheet, and the peak velocity of the electron flow is estimated to be about eight Alfvén speed.

1. Introduction

Magnetic reconnection, which converts magnetic energy into plasma kinetic energy including bulk kinetic energy and thermal energy (Ji et al., 2022; Q. Lu et al., 2022; Parker, 1957; Sweet, 1958; Yamada et al., 2010), has been observed ubiquitously in the solar atmosphere (Lazarian & Desiati, 2010; Lin & Forbes, 2000; Tsuneta, 1995), interplanetary space (Phan et al., 2006; Wang et al., 2023), planetary magnetospheres (Angelopoulos et al., 2008; Burch et al., 2016; Q. Lu et al., 2024; Nagai et al., 2001; Zhang et al., 2012), and laboratory plasma (Egedal et al., 2005; Ji et al., 1998; Olson et al., 2016; Sang et al., 2022; Stenzel & Gekelman, 1981; Yamada et al., 2014). It is generally accepted that magnetic reconnection provides the underlying mechanism that governs explosive phenomena in space environment, like solar flare and substorm. The motion between ions and electrons is decoupled during magnetic reconnection occurring in space plasma (Birn & Hesse, 2001; Divin et al., 2012; Pritchett, 2001; Shay et al., 2001; Wang et al., 2010), which is usually collisionless. The resulted Hall effect leads to the multi-scale structure of diffusion region: an electron diffusion region (EDR) with the scale of electron inertial length is embedded in an ion diffusion region (IDR) with the scale of ion inertial length. In the EDR, both ions and electrons are unmagnetized, whereas in the IDR, ions remain unmagnetized while electrons are magnetized (Birn & Hesse, 2001; Burch et al., 2016; Q. Lu et al., 2010; Pritchett, 2001; Zhou et al., 2019; Zong & Zhang, 2018).

In the IDR, the electrons move toward the X line around the separatrices, and then leave away from the X line along the magnetic field lines just inside the separatrices after they are accelerated by the reconnection electric field in the EDR (Cassak et al., 2017; Drake et al., 2005; Fu et al., 2006; Y.-H. Liu et al., 2017; D. Liu et al., 2021). The generated in-plane Hall current generates the Hall magnetic field in the out-of-plane direction (Birn &
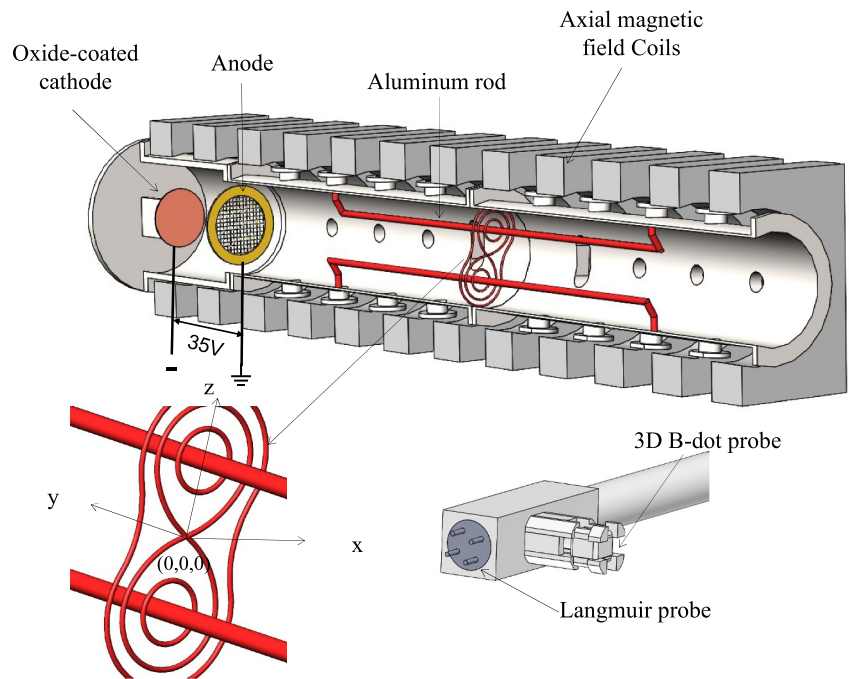
Figure 1. Schematic of the Keda linear magnetized plasma device.

Hesse, 2001; Divin et al., 2012; Q. Lu et al., 2010; Nagai et al., 2003; Ren et al., 2005; Terasawa, 1983). In anti-parallel magnetic reconnection, the Hall magnetic field possesses a symmetric quadrupolar structure, and such kind of symmetry can be distorted by the introduction of a guide field (Eastwood et al., 2010; Lai et al., 2015; S. Lu et al., 2011; Pritchett, 2001; Tharp et al., 2013; Zhou et al., 2018). Now, the Hall magnetic field has been regarded as the most salient feature in magnetic reconnection.

Recently, a new kind of magnetic reconnection occurring in a current sheet with the width of electron inertial length has been pervasively observed in the Earth's magnetosphere (Hubbert et al., 2022; S. Lu et al., 2020; Man et al., 2020; Phan et al., 2018; Wang et al., 2018, 2020). Because there is no obvious ion bulk flow and ion heating, such kind of reconnection is referred to electron-only reconnection (Phan et al., 2018; Pyakurel et al., 2019). It may occur inside or between the coherent structures in turbulent plasma when the size of the reconnection domain is smaller or comparable to the ion gyroradius (Guan et al., 2023). Compared with ion-coupled reconnections, electron-only reconnections exhibit a higher reconnection rate (Greess et al., 2022; Guan et al., 2023). However, there is still a debate on the structure of the out-of-plane magnetic field in electron-only reconnection. Laboratory experiments, an essential tool for studying magnetic reconnection, have also been dedicated to investigate electron-only reconnection. Shi et al. (2022) measured electron distribution during electron-only reconnection in the PHAse Space MApping (PHASMA) device, and observed non-Maxwellian electron distributions. In this Letter, we present the measurements of the out-of-plane magnetic field during electron-only reconnection experiments in the Keda Linear Magnetized Plasma (KLMP) device. A quadrupolar structure of the out-of-plane magnetic field, as well as electron heating, are identified in our experiments.

2. Experimental Setup

The schematic of the magnetic reconnection experiments in the KLMP device is shown in Figure 1. The vacuum chamber, which is 2 m long and 25.5 cm in diameter, is surrounded by 12 sets of magnetic coils. At one end of the vacuum chamber, the plasma is generated by a 15 cm diameter oxide-coated cathode source, which works in the pulse discharge mode at a frequency of 1 Hz and pulse length of 15 ms. The magnetic field coils create a uniform axial background magnetic field to confine the plasma and serve as a guide field for magnetic reconnection. There are two parallel 120-cm-long aluminum rods spaced 17 cm apart, which conduct pulse currents in the same direction and produce the reconnection magnetic field. For efficient use of the vertical probe windows, the rods are mounted at a 20-degree angle from the vertical direction.

Here, argon is used as the fill gas and ionized to produce background plasma with typical electron density of $n_e \approx 1 \times 10^{18}$ m^{-3} and electron temperatures of $T_e \approx 5.5$ eV. The mean free path for electron-ion collisions is about 0.25 m, which is on the same order of the characteristic length (a few 0.1 m), so individual electrons transiting the current sheet experience few collisions, that is, the plasma is marginally collisional at most. On the other hand, the effective resistance (the ratio of the out-of-plane electric field and current density in the X-point) is also an important criterion for collisionless magnetic field reconnection. Based on the measured out-of-plane electric field and current density in the X-point, the ratio of the effective resistance to the Spitzer resistance is about 10, which indicates that the resistance term is small and other terms of generalized Ohm's law dominate (Sang et al., 2022). These results can prove that our magnetic reconnection experiments are in a weakly collisional regime.

The system size $L \approx 0.1$ m is much smaller than the ion inertial length $d_i = 1.44$ m, and comparable to the ion cyclotron radius $r_i = 0.068$ m. In addition, the ion gyroperiod $T_{ci} = 437$ μs is much longer than the experimental time $t_c = 20$ μs. These points imply that the ions are unmagnetized, and are not involved in magnetic reconnection directly. Therefore, the magnetic reconnection in the KLMP device is electron-only reconnection.

A probe array is mounted on a two-dimensional (2D) scanning platform and consists of four Langmuir probes and three-dimensional (3D) magnetic probes. The scanning measurement range of the probes is 11 cm × 8 cm with a step size of 0.5 cm, and the sampling frequency is 2 MHz. The plasma parameters measured by probes include plasma density, electron temperature and 3D magnetic field. In addition, the out-of-plane magnetic field of reconnection is usually one order of magnitude smaller than reconnection magnetic field, so a small angle deviation of magnetic probe can lead to inaccurate measurement of out-of-plane magnetic fields. To address this, the 3D magnetic probes were calibrated with the Helmholtz coil which can be turned over in three dimensions, establishing a mapping relationship between the measured values and the real values. This ensures accurate measurement of the out-of-plane magnetic field, which is related to the Hall magnetic field generated during reconnection.

3. Experimental Results

In our experiment, reconnection occurs between the magnetic fields produced by two parallel aluminum rods, where the currents are the same and flow in the y direction. We measure the magnetic field, plasma density and electron temperature in the reconnection plane, while the current density is calculated according to Ampere's law $\mu_0 \boldsymbol{J} = \nabla \times \boldsymbol{B}$. Figure 2 shows (a) the plasma density n, (b) the current density in the y direction j_y, (c) the fluctuating magnetic field in the y direction $\Delta B_y = B_y - B_g$, and (d) the electron temperature T_e at $t = 8.5, 10, 12,$ and 15μs, while the time evolution of the currents in the parallel rods (I_p) and the current in the denoted region of Figure 2b (I_y) is plotted in Figure 2e. The currents in the two parallel rods increase continuously over time, which drives the produced magnetic fields toward the center of the chamber and magnetic reconnection occurs therein. Initially, the out-of-plane current I_y in Figure 2e also increases continuously over time, and the increase become faster during the time period 7 μs $\lesssim t \lesssim$ 8 μs. Magnetic reconnection occurs from about $t = 7$ μs, and the generated reconnection electric field accelerates electrons in the y direction, which results in a faster increase of the out-of-plane current I_y. With the proceeding of magnetic reconnection, the plasma moves away from the X line, and then the plasma density and the current density around the X line begin to decrease after about $t = 10$ μs. During magnetic reconnection, we can also find the formation of a thin current sheet along the separatrix line from the upper left to the lower right, an increase of the temperature in the thin current sheet, and a quadrupolar structure of the fluctuating magnetic field in the y direction.

Figure 3 plots (a) the fluctuating magnetic field in the y direction $\Delta B_y = B_y - B_g$, (b) the current density in the reconnection plane $|j_{\text{plane}}|$, and (c) the electron flow velocity in the reconnection plane $|V_{e,\text{plane}}|$ at $t = 15$ μs, when the amplitude of Hall magnetic field reaches its maximum value. Here, the current density in the reconnection plane is calculated according to Ampere's law $\mu_0 \boldsymbol{J} = \nabla \times \boldsymbol{B}$, and the electron flow velocity in the reconnection plane is estimated with $V_{e,\text{plane}} \approx \frac{j_{\text{plane}}}{en}$. The Hall magnetic field exhibits a distorted quadrupolar structure, which is dominated by the fluctuating magnetic field in the y direction. Consistent with the fluctuating magnetic field in the y direction, there exists strong in-plane current or electron flow around the X line. Electrons flow toward the X line from the upper-left and the lower-right along one pair of the separatrices, as well as from the upper-right and
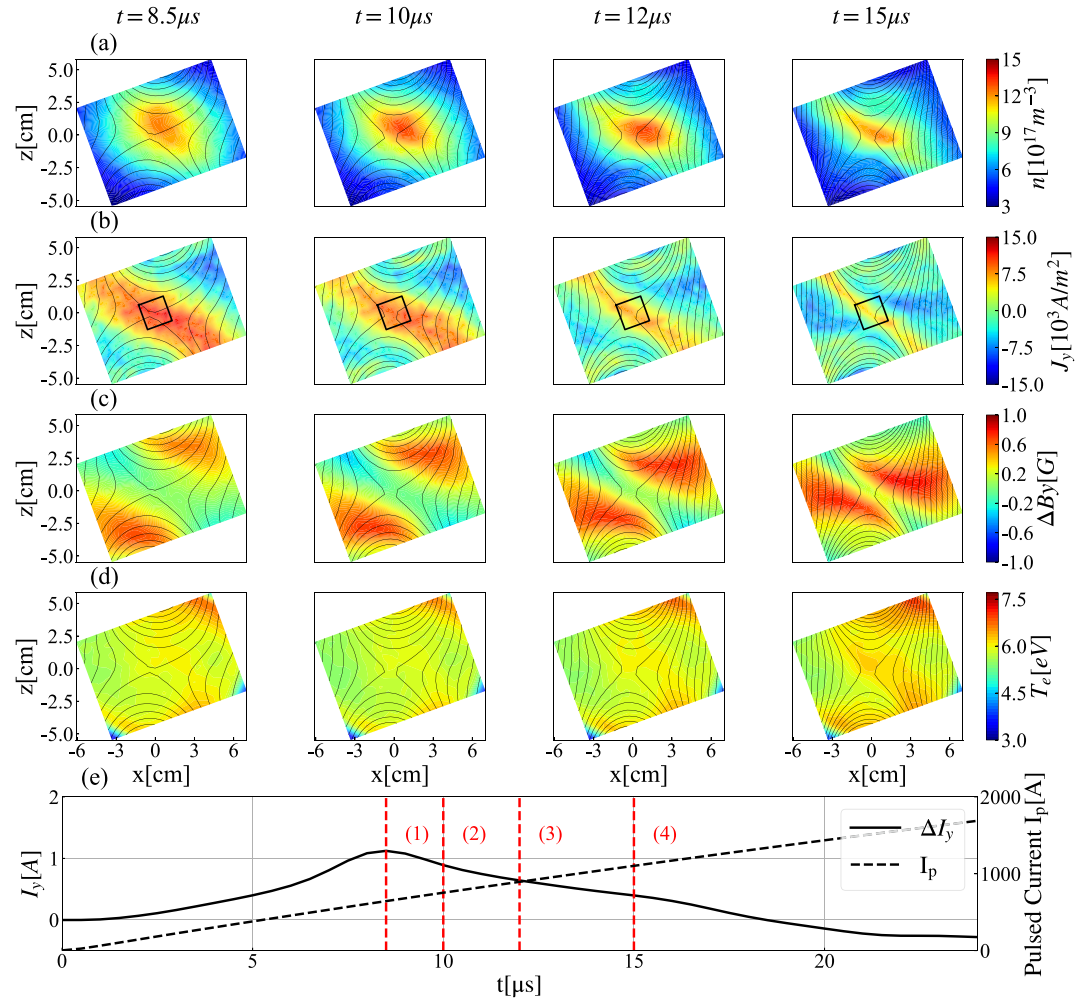
Figure 2. Time evolution of plasma parameters. (a) the plasma density n, (b) the current density in the y direction J_y, (c) the fluctuating magnetic field in the y direction $\Delta B_y = B_y - B_g$, and (d) the electron temperature T_e at $t = 8.5, 10, 12,$ and 15 μs, (e) the currents in the parallel rods (I_p) (black dashed line) and the out-of-plane current I_y in the denoted region of panel (b) with the guide field $B_g = 60$ G, the red dashed line representing the four selected times. The magnetic field lines (solid lines) are also plotted in panels (a)–(d) for reference.
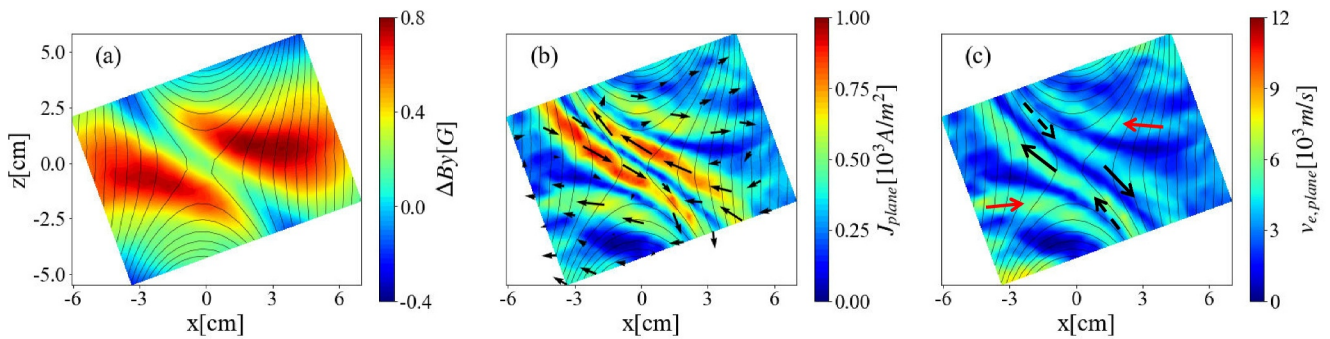
Figure 3. (a) The fluctuating magnetic field in the y direction ΔB_y, (b) the current density in the reconnection plane $|j_{\mathrm{plane}}|$ (the arrows indicate the direction of current density), and (c) the electron flow velocity in the reconnection plane $|V_{e,\mathrm{plane}}| \approx \left|\frac{j_{\mathrm{plane}}}{en}\right|$ (the arrows indicate the direction of electron flow) at $t = 15$ μs. The magnetic field lines (solid lines) are also plotted for reference.
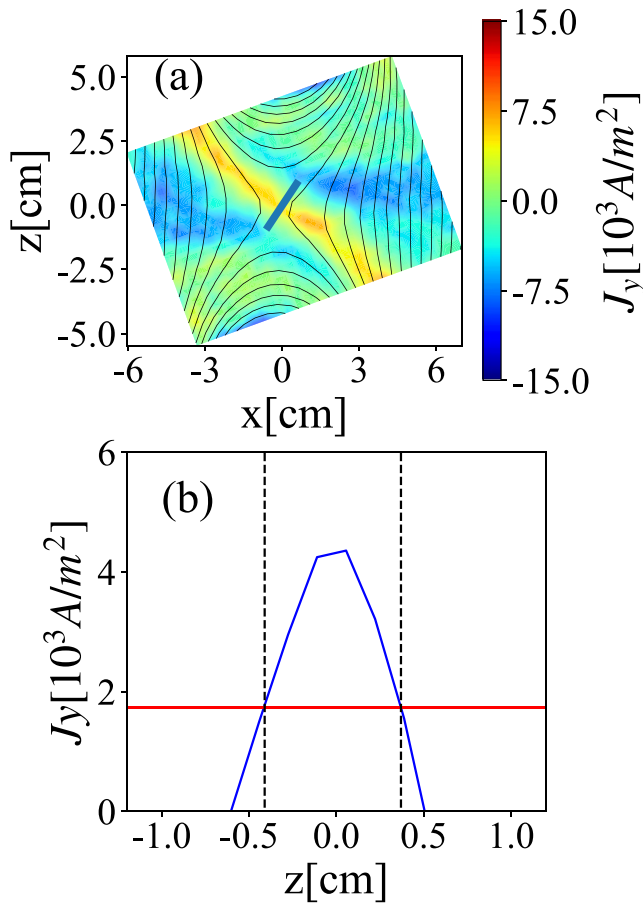
Figure 4. (a) The distribution of current density in the y direction j_y at $t = 15$ μs, and the magnetic field lines (solid lines) are also plotted for reference. (b) The profile of the current density j_y along a line normal to the current sheet at the same time, and the line passes through the X-point. At the red line, the current density reaches 40% of that at the center of the current sheet, and the black dashed lines denote the positions of the half-width of the current sheet.

the lower-left along another pair of the separatrices. After being accelerated around the X line, electrons leave away toward the upper-left and lower-right along the magnetic field lines.

The maximum value of the electron in-plane flow is about 8.1 km/s. In order to calculate the electron flow velocity related to the electron Alfvén speed, we still need to know the asymptotical magnetic field strength B_0. However, the currents in the two parallel aluminum rods increase continuously over the time, and the generated magnetic field is piled up in the upstream of the X line. It is not easy to estimate the asymptotical magnetic field strength B_0.

Figure 4 plots (a) the distribution of current density in the y direction j_y, and (b) the profile of the current density j_y along a line normal to the current sheet (the line passes through the X-point) at $t = 15$ μs. Based on the j_y profiles shown in Figure 4a, we can obtain the position of the half width of the current sheet, and the in-plane magnetic field at the edge of the current sheet is considered as the asymptotic magnetic field. The half-width of the current sheet can be calculated by fitting the profile of the current density in the current sheet with that in the Harris current sheet. In the Harris current sheet, the current density at the half-width is 40% of that at the center. In this way, the magnetic field in the plane at the half-width of the current sheet is about 3 G. The electron Alfvén speed based on the asymptotical magnetic field strength B_0 and the initial plasma density n_0 is about 280 km/s, and the Alfvén speed is about 1 km/s. Consequently, the maximum electron in-plane flow velocity is approximately eight Alfvén speed, yet significantly lower than the electron Alfvén speed.

Based on the profile of the current density j_y in Figure 4b, we can estimate that the half-width of the current sheet is about 0.8 electron inertial length ($d_e \approx 5.3$ mm). Kinetic simulations have shown that the half-width of the current sheet scales with the electron Larmor radius (Roytershteyn et al., 2013). In our experiments, the electron Larmor radius in the guide field is about 1 mm, and then the width of the current layer normalized by the electron Larmor radius is about 4, which is smaller than that observed in MRX (Ji et al., 2008), but similar to that observed in TREX (Greess et al., 2021).

The change in the amplitude of the guide field will affect the distribution of the Hall magnetic field. Figure 5a describes the fluctuating magnetic field ΔB_y and the current density j_y at $t = 7$ μs when the guide field $B_g = 30$ G. At this time, the amplitude of the Hall magnetic field reaches its maximum value. The fluctuating magnetic field ΔB_y also exhibits a quadrupolar structure. Compared to the results with the guide field $B_g = 60$ G, the amplitude of the fluctuating magnetic field ΔB_y becomes larger, and that of the current density j_y is smaller. Figure 5b describes fluctuating magnetic field ΔB_y and the current density j_y with the guide field $B_g = -60$ G at $t = 15$ μs, when the amplitude of Hall magnetic field also reaches its maximum value. Compared to the results with the guide field $B_g = 60$ G, the fluctuating magnetic field ΔB_y changes the direction, and the current density is distributed along the separatrix line from the lower left to the upper right.

4. Conclusions

In this Letter, we report the experimental results of magnetic reconnection with a guide field in the KLMP device. Reconnection occurs between the magnetic fields produced by two parallel aluminum rods, where pulse currents in the same direction are conducted. In our experiment, the ion inertial length is much larger than the diameter of our device, and the ion gyroperiod is much longer than the experimental time. Therefore, we have realized electron-only reconnection in our experiments. By measuring the magnetic field, we find that the out-of-plane magnetic field has a distorted quadrupolar structure, and a thin current sheet with the width of about 0.8 electron inertial length is formed along a pair of separatrix lines. We have also estimated the speed of electron flow in

Figure 5. The fluctuating magnetic field in the y direction ΔB_y and the current density j_y with different guide fields. (a) $B_g = 30$ G at $t = 7$ μs and (b) $B_g = -60$ G at $t = 15$ μs. The magnetic field lines (solid lines) are also plotted for reference.

the reconnection plane, and the maximum value is about 8 Alfvén speed, but much smaller than the electron Alfvén speed. As the reconnection progresses, electron heating occurs on one side of the separation line. The experimental results improve the understanding of electron-only reconnection.

In our experiment, the changes of current density distribution in Figure 2a indicate that the ions still move during the reconnection process. The electron outflow leads to charge separation, and then an electric field is produced (Guan et al., 2024). In the experiments conducted in the VTF device (Egedal et al., 2003, 2007), this strong electric field is found to drive ions to move and change the ion density profile. We plan to further investigate the electron and ion flow driven by in-plane electric fields.

Compared with satellite observations, where physical parameters can only be measured along the satellite trajectory, in magnetic reconnection experiments, these parameters can be obtained at any desired points, which provides us an opportunity to get the whole structure of the out-of-plane magnetic field in electron-only reconnection. At the same time, we can measure the structure of the out-of-plane magnetic field under different current drive conditions, which is helpful to understand the underlying physical mechanisms.

Data Availability Statement

The Experimental data can be downloaded from "National Space Science Data Center, National Science and Technology Infrastructure of China" (Yang, 2024).

References

Angelopoulos, V., McFadden, J. P., Larson, D., Carlson, C. W., Mende, S. B., Frey, H., et al. (2008). Tail reconnection triggering substorm onset. *Science*, *321*(5891), 931–935. https://doi.org/10.1126/science.1160495

Birn, J., & Hesse, M. (2001). Geospace environment modeling (GEM) magnetic reconnection challenge: Resistive tearing, anisotropic pressure and Hall effects. *Journal of Geophysical Research*, *106*(A3), 3737–3750. https://doi.org/10.1029/1999JA001001

Burch, J. L., Torbert, R. B., Phan, T. D., Chen, L.-J., Moore, T. E., Ergun, R. E., et al. (2016). Electron-scale measurements of magnetic reconnection in space. *Science*, *352*(6290), aaf2939. https://doi.org/10.1126/science.aaf2939

Cassak, P. A., Liu, Y.-H., & Shay, M. A. (2017). A review of the 0.1 reconnection rate problem. *Journal of Plasma Physics*, *83*(5), 715830501. https://doi.org/10.1017/S0022377817000666

Divin, A., Lapenta, G., Markidis, S., Semenov, V. S., Erkaev, N. V., Korovinskiy, D. B., & Biernat, H. K. (2012). Scaling of the inner electron diffusion region in collisionless magnetic reconnection. *Journal of Geophysical Research*, *117*(A6), 2011JA017464. https://doi.org/10.1029/2011JA017464

Drake, J. F., Shay, M. A., Thongthai, W., & Swisdak, M. (2005). Production of energetic electrons during magnetic reconnection. *Physical Review Letters*, *94*(9), 095001. https://doi.org/10.1103/PhysRevLett.94.095001

Eastwood, J. P., Shay, M. A., Phan, T. D., & Øieroset, M. (2010). Asymmetry of the ion diffusion region hall electric and magnetic fields during guide field reconnection: Observations and comparison with simulations. *Physical Review Letters*, *104*(20), 205001. https://doi.org/10.1103/PhysRevLett.104.205001

Egedal, J., Fasoli, A., & Nazemi, J. (2003). Dynamical plasma response during driven magnetic reconnection. *Physical Review Letters*, *90*(13), 135003. https://doi.org/10.1103/PhysRevLett.90.135003

Egedal, J., Fox, W., Katz, N., Porkolab, M., Reim, K., & Zhang, E. (2007). Laboratory observations of spontaneous magnetic reconnection. *Physical Review Letters*, *98*(1), 015003. https://doi.org/10.1103/PhysRevLett.98.015003

Egedal, J., Fox, W., Porkolab, M., & Fasoli, A. (2005). Eigenmode response to driven magnetic reconnection in a collisionless plasma. *Physics of Plasmas*, *12*(5), 052107. https://doi.org/10.1063/1.1898205

Fu, X. R., Lu, Q. M., & Wang, S. (2006). The process of electron acceleration during collisionless magnetic reconnection. *Physics of Plasmas*, *13*(1), 012309. https://doi.org/10.1063/1.2164808

Greess, S., Egedal, J., Stanier, A., Daughton, W., Olson, J., Lê, A., et al. (2021). Laboratory verification of electron-scale reconnection regions modulated by a three-dimensional instability. *Journal of Geophysical Research: Space Physics*, *126*(7), e2021JA029316. https://doi.org/10.1029/2021JA029316

Greess, S., Egedal, J., Stanier, A., Olson, J., Daughton, W., Lê, A., et al. (2022). Kinetic simulations verifying reconnection rates measured in the laboratory, spanning the ion-coupled to near electron-only regimes. *Physics of Plasmas*, *29*(10), 102103. https://doi.org/10.1063/5.0101006

Guan, Y., Lu, Q., Lu, S., Huang, K., & Wang, R. (2023). Reconnection rate and transition from ion-coupled to electron-only reconnection. *The Astrophysical Journal*, *958*(2), 172. https://doi.org/10.3847/1538-4357/ad05b8

Guan, Y., Lu, Q., Lu, S., Shu, Y., & Wang, R. (2024). Role of ion dynamics in electron-only magnetic reconnection. *Geophysical Research Letters*, *51*(19), e2024GL110787. https://doi.org/10.1029/2024GL110787

Hubbert, M., Russell, C. T., Qi, Y., Lu, S., Burch, J. L., Giles, B. L., & Moore, T. E. (2022). Electron-only reconnection as a transition phase from quiet magnetotail current sheets to traditional magnetotail reconnection. *Journal of Geophysical Research: Space Physics*, *127*(3), e2021JA029584. https://doi.org/10.1029/2021JA029584

Ji, H., Daughton, W., Jara-Almonte, J., Le, A., Stanier, A., & Yoo, J. (2022). Magnetic reconnection in the era of exascale computing and multiscale experiments. *Nature Reviews Physics*, *4*(4), 263–282. https://doi.org/10.1038/s42254-021-00419-x

Ji, H., Ren, Y., Yamada, M., Dorfman, S., Daughton, W., & Gerhardt, S. P. (2008). New insights into dissipation in the electron layer during magnetic reconnection. *Geophysical Research Letters*, *35*(13), 2008GL034538. https://doi.org/10.1029/2008GL034538

Ji, H., Yamada, M., Hsu, S., & Kulsrud, R. (1998). Experimental test of the Sweet-Parker model of magnetic reconnection. *Physical Review Letters*, *80*(15), 3256–3259. https://doi.org/10.1103/physrevlett.80.3256

Lai, X.-S., Zhou, M., Deng, X.-H., Li, T.-M., & Huang, S.-Y. (2015). How does the guide field affect the asymmetry of hall magnetic and electric fields in fast magnetic reconnection? *Chinese Physics Letters*, *32*(9), 095202. https://doi.org/10.1088/0256-307X/32/9/095202

Lazarian, A., & Desiati, P. (2010). Magnetic reconnection as the cause of cosmic ray excess from the heliospheric tail. *The Astrophysical Journal*, *722*(1), 188–196. https://doi.org/10.1088/0004-637X/722/1/188

Lin, J., & Forbes, T. G. (2000). Effects of reconnection on the coronal mass ejection process. *Journal of Geophysical Research*, *105*(A2), 2375–2392. https://doi.org/10.1029/1999JA900477

Liu, D., Huang, K., Lu, Q., Lu, S., Wang, R., Ding, W., & Wang, S. (2021). The evolution of collisionless magnetic reconnection from electron scales to ion scales. *The Astrophysical Journal*, *922*(1), 51. https://doi.org/10.3847/1538-4357/ac2900

Liu, Y.-H., Hesse, M., Guo, F., Daughton, W., Li, H., Cassak, P. A., & Shay, M. A. (2017). Why does steady-state magnetic reconnection have a maximum local rate of order 0.1? *Physical Review Letters*, *118*(8), 085101. https://doi.org/10.1103/PhysRevLett.118.085101

Lu, Q., Fu, H., Wang, R., & Lu, S. (2022). Collisionless magnetic reconnection in the magnetosphere. *Chinese Physics B*, *31*(8), 089401. https://doi.org/10.1088/1674-1056/ac76ab

Lu, Q., Guo, A., Yang, Z., Wang, R., Lu, S., Chen, R., & Gao, X. (2024). Upstream plasma waves and downstream magnetic reconnection at a reforming quasi-parallel shock. *The Astrophysical Journal*, *964*(1), 33. https://doi.org/10.3847/1538-4357/ad2456

Lu, Q., Huang, C., Xie, J., Wang, R., Wu, M., Vaivads, A., & Wang, S. (2010). Features of separatrix regions in magnetic reconnection: Comparison of 2-D particle-in-cell simulations and Cluster observations. *Journal of Geophysical Research*, *115*(A11), 2010JA015713. https://doi.org/10.1029/2010JA015713

Lu, S., Lu, Q., Cao, Y., Huang, C., Xie, J., & Wang, S. (2011). The effects of the guide field on the structures of electron density depletions in collisionless magnetic reconnection. *Chinese Science Bulletin*, *56*(1), 48–52. https://doi.org/10.1007/s11434-010-4250-9

Lu, S., Wang, R., Lu, Q., Angelopoulos, V., Nakamura, R., Artemyev, A. V., et al. (2020). Magnetotail reconnection onset caused by electron kinetics with a strong external driver. *Nature Communications*, *11*(1), 5049. https://doi.org/10.1038/s41467-020-18787-w

Man, H. Y., Zhou, M., Yi, Y. Y., Zhong, Z. H., Tian, A. M., Deng, X. H., et al. (2020). Observations of electron-only magnetic reconnection associated with macroscopic magnetic flux ropes. *Geophysical Research Letters*, *47*(19), e2020GL089659. https://doi.org/10.1029/2020GL089659

Nagai, T., Shinohara, I., Fujimoto, M., Hoshino, M., Saito, Y., Machida, S., & Mukai, T. (2001). Geotail observations of the Hall current system: Evidence of magnetic reconnection in the magnetotail. *Journal of Geophysical Research*, *106*(A11), 25929–25949. https://doi.org/10.1029/2001JA900038

Nagai, T., Shinohara, I., Fujimoto, M., Machida, S., Nakamura, R., Saito, Y., & Mukai, T. (2003). Structure of the hall current system in the vicinity of the magnetic reconnection site. *Journal of Geophysical Research*, *108*(A10), 2003JA009900. https://doi.org/10.1029/2003JA009900

Olson, J., Egedal, J., Greess, S., Myers, R., Clark, M., Endrizzi, D., et al. (2016). Experimental demonstration of the collisionless plasmoid instability below the ion kinetic scale during magnetic reconnection. *Physical Review Letters*, *116*(25), 255001. https://doi.org/10.1103/PhysRevLett.116.255001

Parker, E. N. (1957). Sweet's mechanism for merging magnetic fields in conducting fluids. *Journal of Geophysical Research*, *62*(4), 509–520. https://doi.org/10.1029/JZ062i004p00509

Phan, T. D., Eastwood, J. P., Shay, M. A., Drake, J. F., Sonnerup, B. U. Ö., Fujimoto, M., et al. (2018). Electron magnetic reconnection without ion coupling in Earth's turbulent magnetosheath. *Nature*, *557*(7704), 202–206. https://doi.org/10.1038/s41586-018-0091-5

Phan, T. D., Gosling, J. T., Davis, M. S., Skoug, R. M., Øieroset, M., Lin, R. P., et al. (2006). A magnetic reconnection X-line extending more than 390 Earth radii in the solar wind. *Nature*, *439*(7073), 175–178. https://doi.org/10.1038/nature04393

Pritchett, P. L. (2001). Geospace Environment Modeling magnetic reconnection challenge: Simulations with a full particle electromagnetic code. *Journal of Geophysical Research*, *106*(A3), 3783–3798. https://doi.org/10.1029/1999JA001006

Pyakurel, S. P., Shay, M. A., Phan, T. D., Matthaeus, W. H., Drake, J. F., TenBarge, J. M., et al. (2019). Transition from ion-coupled to electron-only reconnection: Basic physics and implications for plasma turbulence. *Physics of Plasmas*, *26*(8), 082307. https://doi.org/10.1063/1.5090403

Ren, Y., Yamada, M., Gerhardt, S., Ji, H., Kulsrud, R., & Kuritsyn, A. (2005). Experimental verification of the hall effect during magnetic reconnection in a laboratory plasma. *Physical Review Letters*, *95*(5), 055003. https://doi.org/10.1103/PhysRevLett.95.055003

Roytershteyn, V., Dorfman, S., Daughton, W., Ji, H., Yamada, M., & Karimabadi, H. (2013). Electromagnetic instability of thin reconnection layers: Comparison of three-dimensional simulations with MRX observations. *Physics of Plasmas*, *20*(6), 061212. https://doi.org/10.1063/1.4811371

Sang, L., Lu, Q., Xie, J., Fan, F., Zhang, Q., Ding, W., et al. (2022). Energy dissipation during magnetic reconnection in the Keda linear magnetized plasma device. *Physics of Plasmas*, *29*(10), 102108. https://doi.org/10.1063/5.0090790

Shay, M. A., Drake, J. F., Rogers, B. N., & Denton, R. E. (2001). Alfvénic collisionless magnetic reconnection and the hall term. *Journal of Geophysical Research*, *106*(A3), 3759–3772. https://doi.org/10.1029/1999JA001007

Shi, P., Srivastav, P., Barbhuiya, M. H., Cassak, P. A., Scime, E. E., & Swisdak, M. (2022). Laboratory observations of electron heating and non-Maxwellian distributions at the kinetic scale during electron-only magnetic reconnection. *Physical Review Letters*, *128*(2), 025002. https://doi.org/10.1103/PhysRevLett.128.025002

Stenzel, R. L., & Gekelman, W. (1981). Magnetic field line reconnection experiments 1. Field topologies. *Journal of Geophysical Research*, *86*(A2), 649–658. https://doi.org/10.1029/JA086iA02p00649

Sweet, P. A. (1958). The neutral point theory of solar flares. In *Symposium—International Astronomical Union* (Vol. 6, pp. 123–134). https://doi.org/10.1017/S0074180900237704

Terasawa, T. (1983). Hall current effect on tearing mode instability. *Geophysical Research Letters*, *10*(6), 475–478. https://doi.org/10.1029/GL010i006p00475

Tharp, T. D., Yamada, M., Ji, H., Lawrence, E., Dorfman, S., Myers, C., et al. (2013). Study of the effects of guide field on Hall reconnection. *Physics of Plasmas*, *20*(5), 055705. https://doi.org/10.1063/1.4805244

Tsuneta, S. (1995). Structure and dynamics of magnetic reconnection in a solar flare. *The Astrophysical Journal*, *456*, 840. https://doi.org/10.1086/176701

Wang, R., Lu, Q., Huang, C., & Wang, S. (2010). Multispacecraft observation of electron pitch angle distributions in magnetotail reconnection. *Journal of Geophysical Research: Space Physics*, *115*(A1), 2009JA014553. https://doi.org/10.1029/2009JA014553

Wang, R., Lu, Q., Lu, S., Russell, C. T., Burch, J. L., Gershman, D. J., et al. (2020). Physical implication of two types of reconnection electron diffusion regions with and without ion-coupling in the magnetotail current sheet. *Geophysical Research Letters*, *47*(21), e2020GL088761. https://doi.org/10.1029/2020GL088761

Wang, R., Lu, Q., Nakamura, R., Baumjohann, W., Huang, C., Russell, C. T., et al. (2018). An electron-scale current sheet without bursty reconnection signatures observed in the near-Earth tail. *Geophysical Research Letters*, *45*(10), 4542–4549. https://doi.org/10.1002/2017GL076330

Wang, R., Yu, X., Wang, Y., Lu, Q., & Lu, S. (2023). Observation of the hall magnetic reconnection as close as 56 solar radii from the Sun. *The Astrophysical Journal*, *947*(2), 78. https://doi.org/10.3847/1538-4357/acbdf6

Yamada, M., Kulsrud, R., & Ji, H. (2010). Magnetic reconnection. *Reviews of Modern Physics*, *82*(1), 603–664. https://doi.org/10.1103/RevModPhys.82.603

Yamada, M., Yoo, J., Jara-Almonte, J., Ji, H., Kulsrud, R. M., & Myers, C. E. (2014). Conversion of magnetic energy in the magnetic reconnection layer of a laboratory plasma. *Nature Communications*, *5*(1), 4774. https://doi.org/10.1038/ncomms5774

Yang, F. (2024). Data for "Laboratory Observations of Hall magnetic field in electron-only magnetic reconnection with a guide field" [Dataset]. *Science Data Bank*. https://doi.org/10.57760/sciencedb.18086

Zhang, T. L., Lu, Q. M., Baumjohann, W., Russell, C. T., Fedorov, A., Barabash, S., et al. (2012). Magnetic reconnection in the near Venusian magnetotail. *Science*, *336*(6081), 567–570. https://doi.org/10.1126/science.1217013

Zhou, M., El-Alaoui, M., Lapenta, G., Berchem, J., Richard, R. L., Schriver, D., & Walker, R. J. (2018). Suprathermal electron acceleration in a reconnecting magnetotail: Large-scale kinetic simulation. *Journal of Geophysical Research: Space Physics*, *123*(10), 8087–8108. https://doi.org/10.1029/2018JA025502

Zhou, M., Man, H. Y., Zhong, Z. H., Deng, X. H., Pang, Y., Huang, S. Y., et al. (2019). Sub-ion-scale dynamics of the ion diffusion region in the magnetotail: MMS observations. *Journal of Geophysical Research: Space Physics*, *124*(10), 7898–7911. https://doi.org/10.1029/2019JA026817

Zong, Q.-G., & Zhang, H. (2018). In situ detection of the electron diffusion region of collisionless magnetic reconnection at the high-latitude magnetopause. *Earth and Planetary Physics*, *2*(3), 1–7. https://doi.org/10.26464/epp2018022